DETECTION OF CAVITATION BY ACOUSTIC AND VIBRATION-MEASUREMENT METHODS

BY J. J. VARGA *, G. SEBESTYEN **
AND A. FAY ***

I. — Introduction

It is a well-known fact that cavitation in hydraulic machines is always associated with vibration and noise phenomena. Their character and intensity depends on the cavitation conditions. The observation of cavitation in hydraulic machines was possible only visually so far (through a transparent wall or window, by using mostly stroboscope illumination), which was relatively easy to realize in case of small-size machines or models, if only to a limited extent, but which presented difficulties or was often entirely impossible when large-size machines had to be tested. For this reason, particularly in the last decade, acoustic investigations were thrust into prominence as the noise and/or vibration associated with cavitation seemed suitable for the detection of cavitation phenomena encountered in places inaccessible for visual observation.

Although the hitherto investigations lead to the conclusion that the incipient cavitation is most sensitively indicated by the rapid increase of noise [1-4], still no generally accepted method has been developed, as yet, for its measurement. The measurements performed in this direction so far covered various frequency ranges and made use of different instruments [5, 6], thus the cavitation inception was determined also by means of different methods. The similarity of the results of investigations, however, confirms the adaptability of the test method in question.

The noise investigations at various cavitating conditions operating hydraulic machines was, due to the complex character of the problem, only scarcely employed owing, above all, to the uncertainties discovered in the measurements techniques.

With the simple and readily reproducible noise and vibration measurement method [7] elaborated in course of the cavitation research work conducted by the Department of Hydraulic Machinery of the Budapest Technical University applied to models located in closed circuit cavitation tunnel [8], pumps [9, 10], and a Francis turbine model [11], the results of completed test procedures verified the adaptability of this method. The following paragraphs present the results obtained so far, and the conclusions arrived at therefrom.

II. — Description of the measuring equipment

The vibrations produced by cavitation, and the intensity of the noise emitted were measured by using a Brüel and Kjaer condenser microphone adaptable within the frequency range of 20 to 40 000 cps, an accelerometer for measurements within the frequency range of 2 to 25 000 cps, the necessary amplifiers, a frequency analyzer operating in the 20 to 20 000 cps range, and an automatic level recorder suitable for the registration of variable voltage le-

* Professor, Department of Hydraulic Machinery, Budapest Technical University (Hungary).

** Research Engineer, Department of Hydraulic Machinery, Budapest Technical University (Hungary).

*** Mech. Eng., Math., Department of Hydraulic Machinery, Budapest Technical University, and Ganz-Mavag Co, Budapest (Hungary).

Article published by SHF and available at http://www.shf-lhb.org or http://dx.doi.org/10.1051/lhb/1969012

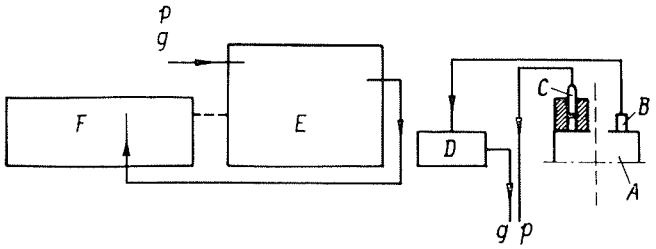

1/ Schematic diagram of the instrumentation used for noise measurements. A : the object tested; B : accelerometer; C : condenser microphone; D : pre-amplifier; E : frequency analyser; F : level recorder; *g* : accelerometer cable; *p* : microphone cable.

Schéma de principe des appareils employés pour les mesures acoustiques. A : objet étudié; B : accéléromètre; C : microphone à capacitance; D : pré-amplificateur; E : analyseur de fréquence; F : enregistreur de niveau; g : *câble de l'accéléromètre;* p : *câble du microphone.*

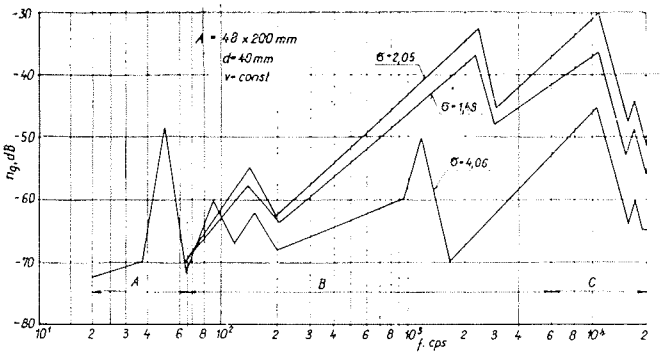

2/ Acceleration level n_g in the function of frequency f, with different cavitation numbers σ, in case of a $d = 48$ mm diameter circular cylinder model located in a test section of $A = 48 \times 200$ mm.

Niveau d'accélération n_g *en fonction de la fréquence* f *et de l'indice de cavitation* σ *pour le cas d'un modèle de cylindre circulaire de diamètre 48 mm, dans une section expérimentale A égale à* 48×200 *mm.*

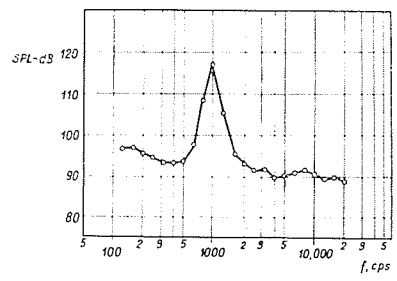

3/ Sound pressure level SPL in function of frequency, on the basis of experiments conducted by Etkin et al. [13] with air, at a velocity of $v = 225$ ft/sec. using a $d = 1/2''$ cylinder model in a $48'' \times 32''$ test section.

Niveau de pression sonore SPL en fonction de la fréquence, sur la base d'expériences faites par Etkin et al. [13] avec de l'air, à la vitesse $v = 225$ *pieds/s; modèle cylindrique* $d = 1/2''$ *dans une section expérimentale de* $48'' \times 32''$.

vel values (Fig. 1). The advantages of this method are that no window is required on the housing of the machine tested, and the equipment is simple and portable. It has the disadvantage of a limited frequency range which is, nevertheless, sufficient for the larger bubble sizes [12].

In the experiments, the accelerometer was mounted onto the object to be measured while the microphone was located in the vicinity of the machine or working section under test, possibly isolated from all external noises. The acoustic measurements performed with the capacitor microphone determined sound pressure level values whereas the vibration measurements informed on acceleration or, more precisely, acceleration level values.

The noise measurements associated with hydraulic investigations were performed with the systems listed above. Thus various models placed perpendicular to the direction of the flow in the working chamber of the closed circuit hydrodynamic tunnel [8] and those similarly in a closed type turbine model test rig with resorbers where, in course of turbine model studies, the cavitation was visually observed and the various types were photographied, have been made use of [11]. Experiments were conducted, in open circuits furthermore, on a pump with semi open impeller (without front shroud) for the visual observation of cavitation and, both in closed and open systems, with pumps where no visual observation was feasible [9, 10].

The various hydraulic investigations (in hydrodynamic tunnel, pumps, turbine) employed the cavitation numbers corresponding to the given conditions. In turbine investigations, the cavitation number was calculated with the static suction head and net head taken into account, in pump tests the Thoma cavitation number was accounted using the total energy of the liquid upstream the impeller, and the reference delivery head was represented by the value measured under non-cavitating conditions, whereas the investigations on models in a hydrodynamic tunnel employed the pressure and velocity values prevailing at the place of the model producing cavitation, but in its absence, for the calculation of the cavitation factors. These cavitation numbers determined in practice are appropriate for characterizing the various cavitation conditions. Hence the cavitation numbers will be uniformly indicated by sigma which, however, always represents the respective value of those listed above.

III. — Noise spectrum

Noise spectrum means the curve illustrating the relationship of sound pressure level (in vibration measurements: acceleration level) and frequency number. These curves offer useful information for studies of cavitational flow. They make possible the determination of the correlation between the Strouhal number $\mathcal{S}$ and the cavitation number within a given system, and they represent the basis for the acoustic examination of hydraulic machines operating under cavitating conditions.

Figure 2 presents, in simplified outlines, the noise spectrum curves plotted with different cavitation numbers in the 20 to 20 000 cps frequency

range, during measurements on a model located against the flow in the closed circuit hydraulic tunnel. Such curves can be divided into three characteristic sections. The range indicated by A is characterized basically by the noise of the bearings and the auxiliary machines (pump, electromotor and its feeding aggregate). In range B, the effect of the cavitating flow conditions is manifested to different degrees depending on frequency. Finally, in range C, the curves depend only on the cavitation number and run almost parallelly.

This curve run-off is due to the two fundamental noise generators existing in cavitation flow:

a) Noise emitted at a discrete frequency determined by the flow conditions, as the result of the periodic separation of cavitation vortices;

b) Sound radiation produced by bubble collapse at a wide frequency spectrum extended into the supersonic range.

1. The Strouhal number.

On the basis of the first noise source, the frequency of the wakes shedding from the model can be determined from the noise spectrum, that is, from the frequency number pertaining to its peak value. This test method proved to be successful in wind tunnel experiments as well, as attested by the diagram of Figure 3, published originally by Etkin, Korbacher and Keefe [13]. The slowly subsiding curve of the noise spectrum has, at around the frequency number of 1 000 cps, a steeply protruding peak associated with periodic vortex separation, which corresponds to the separation frequency of vortices forming a Karman vortex street.

The periodic vortex separation can be verified and the separation frequency determined, by means of the noise spectrum, under cavitational flow conditions as well. Along the curves plotted in Figure 2, between $60 < f < 200$ cps is the range where the determination of the separation period from the noise level peak points possible. The frequency curve detail presented in Figure 4 reveals that this peak, referring to an *a* type noise generator, protrudes under the given cavitation condition by about 20 dB from the noise level of the surrounding frequencies. Varga and Sebestyén [14, 15] has shown the correlation between Strouhal number and cavitation number using various methods, including noise test for determination, of the frequency of vortices shedding periodically from circular cylinder model. Figure 5 presents the photograph of cavitation bubble clusters separated from wedge model, exposed with a short illumination time. Lecher [16] photographed periodic vortex separation from a turbine blades under cavitating condition.

2. Noise level.

The sections of the noise spectra in the C-range (6 000 ... 20 000 cps) presented in Figure 2 run approximately parallel, that is, the average distance there-between is practically constant. This indicates that, within this range, the relative values are independent of frequency. This nature of the noise spectra is closely connected to the energy emitted over a wide band when the cavitation bubbles collapse (*b*-type noise generator).

Pokrovsky and Yudin [17] obtained identical results in course of their noise investigations conducted on a pump. One of their noise spectrum curves is shown in Figure 6. During his pump and turbine cavitation noise tests, Pearsall [12] measured the sound pressure level values at selected frequencies. Of his characteristic curves, those plotted at the frequencies of 20 000 and 12 500 cps, respectively, are approximately parallel which supports our previous conclusions (Fig. 7).

On grounds of the above peculiar characteristics of the noise spectra, the results of our earlier investigations [8, 11] revealed unequivocally, as confirmed by the papers cited too, that investigations on the cavitation flow phenomena do not require the determination of the total noise spectrum but it is sufficient to select one or, in order to ensure higher accuracy, two frequencies within the specified range (between 6 000 and 20 000 cps), and

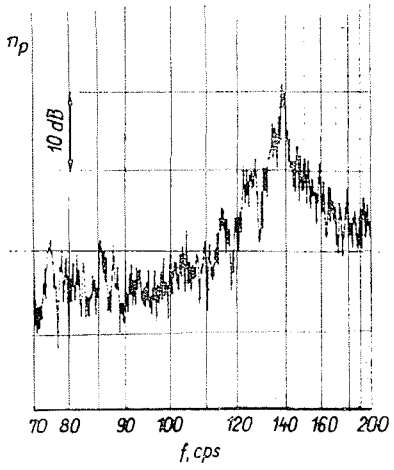

4/ Noise spectrum curve detail (sound pressure level in the function of frequency), plotted for circular cylinder model of $d = 48$ mm diameter, located in the 48×200 mm test section of a closed cavitation tunnel. $\mathcal{R} = 5.29.10^5$, $\sigma = 1.93$.

Détail de la courbe du spectre acoustique (niveau de pression sonore en fonction de la fréquence), correspondant à un modèle de cylindre circulaire de diamètre = 48 mm, installé dans la section expérimentale de 48×200 mm d'un tunnel de cavitation fermé. $\mathcal{R} = 5{,}29.10^4$; $\sigma = 1{,}93$.

5/ Photograph of a cavitation vortex separated from the model. Illumination period $\tau = 10^{-5}$ sec.

Photographie d'un tourbillon de cavitation s'étant décollé du modèle. Durée d'éclairage $\tau = 10^{-5}$ s.

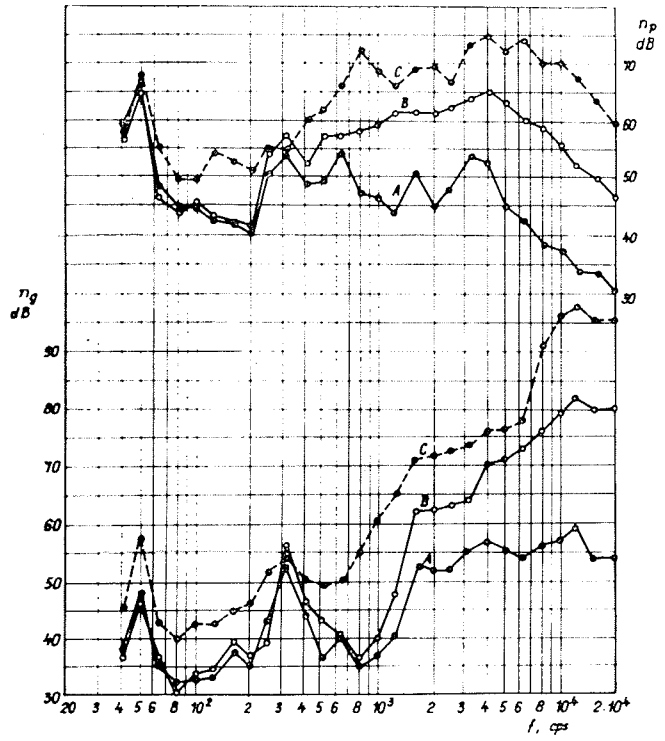

6/ Vibration (lower curves) and noise spectre (upper curves) of a centrifugal pump, in the function of frequency, according to the experiments conducted by Pokrovsky and Yudin [17], under different (A,B,C) cavitation conditions.

Vibrations (courbes inférieures) et spectre acoustique (courbes supérieures) d'une pompe centrifuge, en fonction de la fréquence, selon les expériences de Pokrovsky et Yudin [17] dans des conditions de cavitation variables (A,B,C).

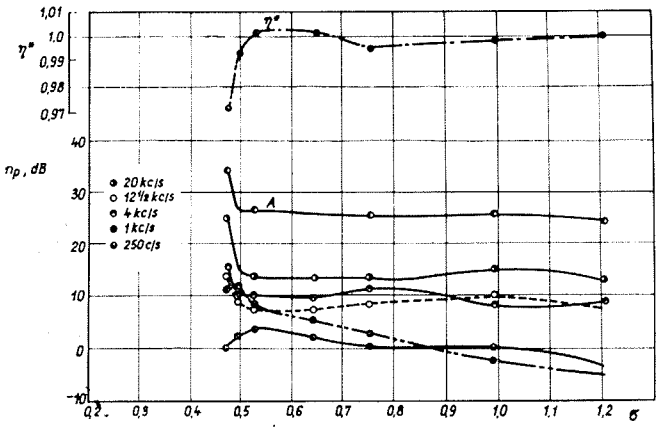

7/ Relative efficiency η^* and sound pressure level n_p in function of the cavitation number σ, according to the experiments conducted by Pearsall [12] with a Kaplan turbine (curve A illustrates the entire sound pressure level).

Rendement relatif η^* et niveau de pression sonore n_p, en fonction du σ de cavitation, selon les expériences de Pearsall [12] faites sur une turbine Kaplan; la courbe A représente l'ensemble du niveau de pression sonore.

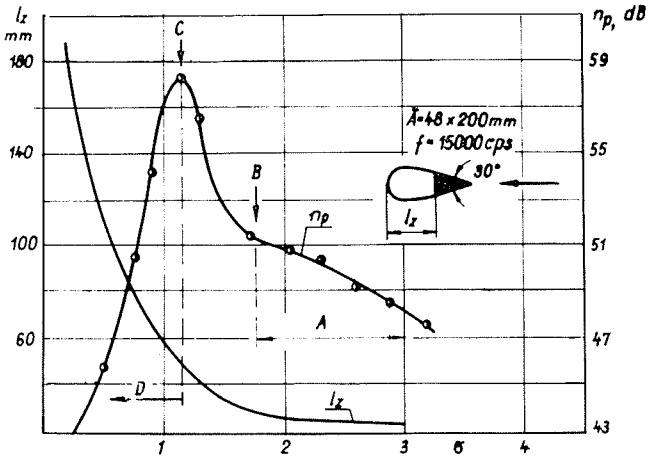

8/ Variation of the sound pressure level n_p and the cavitations zone length l_z, in function of the cavitation number σ, in a 30° wedge model, at a measurement frequency of 15 000 cps. A : appearance of cavitation vortex filaments behind the model, and the development of a short cavitation whisker; B : beginning of the separation of cavitation vortices; C : culmination point; D : exhaustion range.

Variation du niveau de pression sonore n_p et de la longueur de la zone de cavitation l_z en fonction du σ de cavitation : cas d'un modèle de coin à 30°, fréquence de mesure 15 000 Hz. A : apparition de filaments de tourbillon de cavitation à l'aval du modèle et formation d'une courte traînée de cavitation; B : début du décollement des tourbillons de cavitation; C : point culminant du phénomène; D : domaine d'épuisement du phénomène.

perform the measurements thereat, whereby the measuring work will be greatly reduced.

During the measurements, it was advantageous that the determination of the absolute level values was not necessary but it was sufficient to study the differences from the noise level (sound pressure or acceleration) determined under non-cavitating condition. Measurement accuracy was increased by using the mean values determined by the graphical integration of the noise level values recorded in the function of time.

Illustration of the noise level in fuction of the cavitation number σ or relative cavitation zone length λ will be hence called *noise level curve.* The two illustration methods (in fuction of σ or λ) are essentially equivalent because cavity length is a unique function of cavitation number [15, 18].

IV. — The character of noise level curves

In hydraulic machines, cavitation may occur at various places during their operation (blade cavitation, tip clearence cavitation, suction pipe vortex cavitation, etc.). These cavitation phenomena appearing at different points may be encountered simultaneously. The noise thus produced is the composition of the noise phenomena of the diffe-

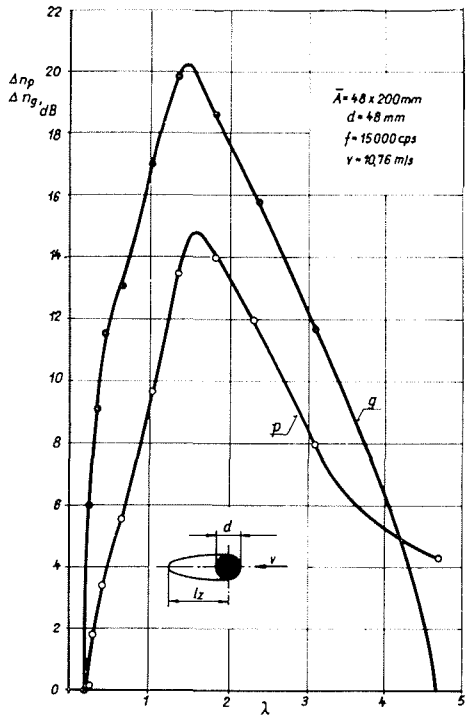

9/ Sound pressure level Δn_p and acceleration level Δn_g differences in function of the relative cavity length $\lambda = l_z/d$, of a circular cylinder model test performed in a hydrodynamic tunnel.

Différences du niveau de pression sonore Δn_p *et du niveau d'accélération* Δn_g *en fonction de la longueur de cavité relative* $\lambda = l_z/d$, *correspondant à un essai effectué avec un modèle de cylindre circulaire en tunnel hydrodynamique.*

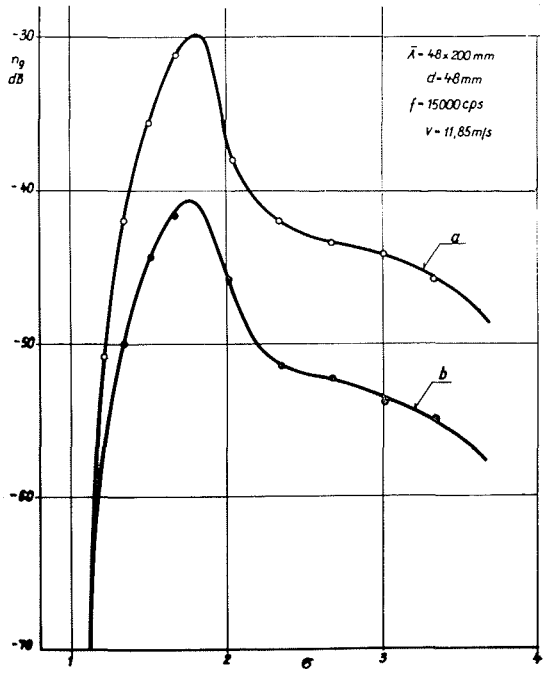

10/ Variation of the acceleration level n_g in function of the cavitation number σ, for a cylinder model in a hydrodynamic tunnel :
a : measurements at the perspex sidewall;
b : measurements at the steel sidewall.

Variation du niveau d'accélération n_g *en fonction du* σ *de cavitation, dans le cas d'un modèle de cylindre circulaire dans un tunnel hydrodynamique :*
a : *mesures à la paroi latérale en plexiglass;*
b : *mesures à la paroi latérale en acier.*

rent type cavitation phenomena produced at the different places. In order to arrive at conclusions from these complex noise phenomena, it is necessary to be familiar with the test results of the individual cavitation phenomena. Such individually produced, isolated cavitation phenomenon is, for example, that produced behind a model located in a hydrodynamic tunnel.

1. Noise level curves of isolated cavitation.

Noise level curves of wedge-shape and cylindrical models located against the flow in closed hydrodynamic tunnel were plotted by using condenser microphone placed next to the test sections, and accelerometers mounted onto the sidewalls thereof. To facilitate the visual observation three sidewalls of the test section were made of transparent material (perspex), while the fourth one of steel. Acceleration level was measured by accelerometers mounted on both the persplex and steel walls. The measurements rendered identical results.

In case of an isosceles wedge model of a 30° apex angle, the relationship between cavitation number, sound pressure level, and cavity length respectively, is illustrated by Figure 8, where the noise level of a complete cavitation process (inception, development, and gradual exhaustion of cavitation), as measured at 15 000 cps frequency, is recorded. Cavitation development is characterized by the cavitation number range wherein the noise level is increasing with decreasing cavitation number. Where, on the other hand, the noise level is decreasing, the intensity of cavitation will similarly decrease. In the cavitation number range of the diagram marked by A, along the lower and upper side of the model, respectively, the diminution of the cavitation number leads to the development of a gradually increasing cavitation cloud indicated by the increased noise level as well. Separation of the vortices begins in point B whence the noise level is steeply increasing up to point C where cavitation is of a maximum intensity, and the intensity of the emitted sound has similarly a maximum value. This is followed (in zone marked by D) by the development of a pulsating cavitation zone of much less intensity with, finally, the intensity completely lost, that is, exhausted.

The results of investigation with circular cylinder models are presented in Figures 9, 10 and 11, whereas Figure 12 illustrates the results of sound pressure and acceleration level measurements performed on a pump, in order to verify that the character of the noise level curves is independent, within the suitably selected frequency range, of the frequency number and the method of (noise or acceleration level measurement) observation. Further peculiar characteristics of the noise level curves presented in this Figure will be dealt with by Section IV. 3 in detail.

Figure 13 displays noise level curves plotted for an wedge model at various flow velocities, which

lead to the conclusion that the different stress conditions of the test section walls, produced by the different pressures, and the Reynolds number exert only a negligible influence with respect to the noise level curves.

Figure 14 was plotted by making use of the data (Fig. 18, 23, 24 and 30) offered by a publication [19] reporting on the extensive noise investigations conducted by Numachi on blade profiles. This Figure presents the noise level curves of the $\alpha = 0°$ incidence angle Clark profile, pertaining to different frequency values, and the relative cavity lengths in function of the cavitation index (using author's symbols). The character of these noise level curves is identical to that of the curves presented above. The cavitation index $k_d = 1.12$ represents, according to the author, the condition immediately preceding cavitation inception.

Summarizing the diagrams presented, it may be stated that the character of the noise level curves (that is, the variation of the ascending and descending sections, and the location of peaks) is governed to a decisive extent by the cavitating conditions and their variations. With other words, the noise level curves are affected only to an insignificant degree by the value of the frequency optionally selected from the frequency range suitable for the test, by the relative position of the sensing device, the material of the walls limiting the flow, and by the sensing method (sound pressure or acceleration measurement). All these were confirmed also by the results of hydraulic machine tests described below.

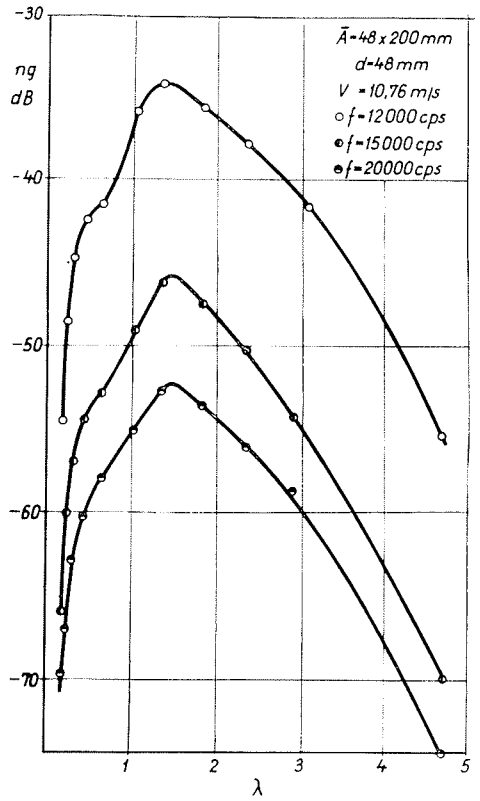

11/ Variation of the acceleration level n_g in function of the relative cavity length λ, for a cylindrical model, at different frequencies.

Variation du niveau d'accélération n_g *en fonction de la longueur de cavité relative* λ, *dans le cas d'un modèle cylindrique et avec des fréquences variables.*

2. Noise level curves of model turbine.

The acustic method described above was employed for the cavitation noise test of a Francis turbine model of $n_s = 100$ metric specific speed. The noise spectrum measurements were performed with the condenser microphone located on the wall of the draft tube. These measurements confirmed the earlier findings and, therefore, the subsequent noise level measurements involved the same frequency ($f = 15\,000$ cps). Figure 15 presents a noise level curve plotted for an operating condition near to the best efficiency point at full opening. It is conspicuous that not only the noise level curve presented but all noise level curves measured under other operational conditions have similarly two peak values. The correlation between the cavitation developed in the turbine and the noise level curve can be readily analyzed on the basis of this Figure.

On grounds of visually observed cavitation forms, their photographs, the results of output characteristic measurements, and their comparison to the noise level curve data, the following statements may be made:

In the measurements discussed, the first symptom of cavitation upon the gradual reduction of the cavitation number could be observed along the centre line of the runner (at $\sigma = 0{,}54$ value). However, the noise level curve started to ascend as early as at the value of $\sigma = 0{,}6$ which refers to an earlier inception of the cavitation but impossible to observe visually, as yet. Hammitt [4] reported from similar observation. With the cavitation thus started, the further reduction of the cavitation number led to the development of a funnel shape vortex cavitation along the centre line of the turbine, and to the simultaneous increase of the noise level. With further reduced cavitation numbers, the cavitation funnel grew longer and thicker (Fig. 16) penetrating, finally, into the suction bend whereby the cavitation condition became to resemble that called blocking in cavitation tunnels, characterized theoretically by an "infinite" cavitation wake. Above the value of $\sigma = 0{,}25$ no blade cavitation symptoms could be observed, thus the development of the noise level curve was influenced by the cavitation funnel alone. In this section, the course of the noise level curve is similar to that obtained under isolated cavitation test conditions, including the development and exhaustion stages.

The first symptoms of blade cavitation were observed at a $\sigma = 0{,}13$ values. The noise level curve will, however, ascend as soon as at $\sigma = 0{,}20$ which refers to the actual inception of the blade cavitation, indicated by the slight modification of water discharge and speed as well. At such cavitation numbers, the cavitation noise is produced by the super-imposition of the blade cavitation and vortex cavitation noises. The sudden rise of noise level may be attributed to the effect of blade cavitation and with the output characteristic changes takes into account, the inception of blade cavitation may be assumed at the $\sigma_i = 0{,}28$ value. The noise produced by the vortex cavitation may be neglect-

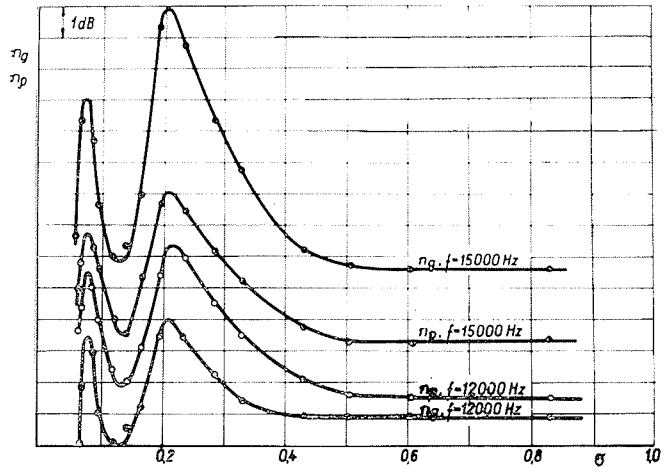

12/

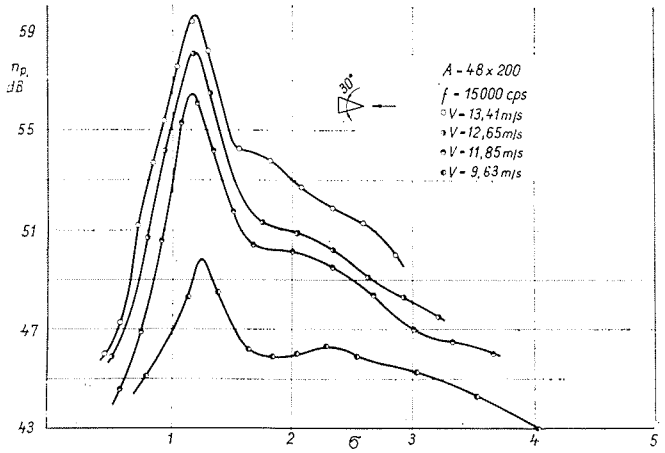

13/

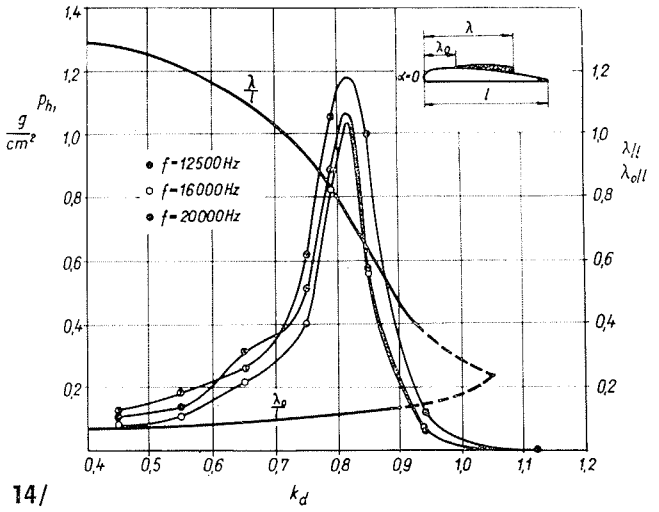

14/

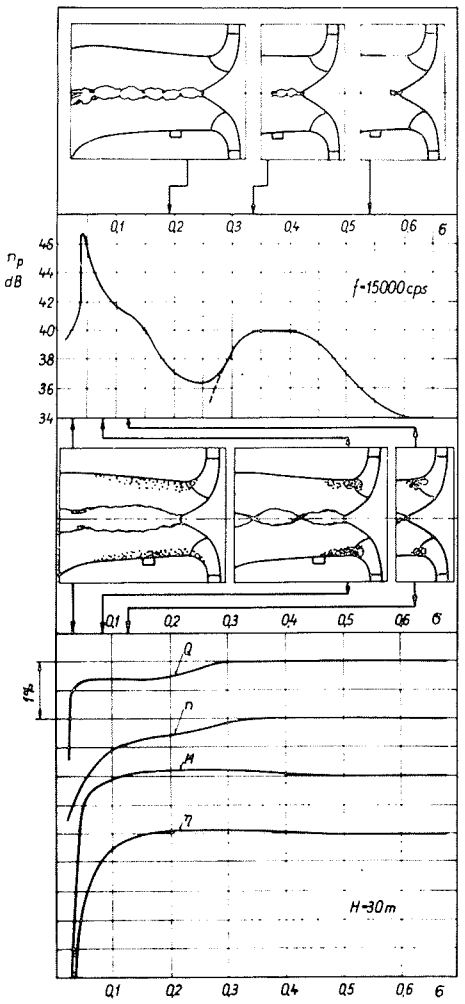

15/

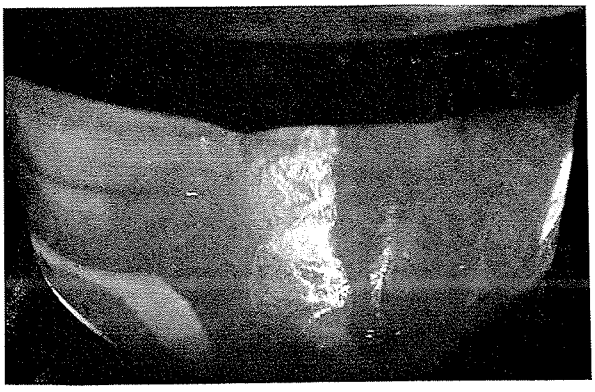

16/

12/ Variation of the acceleration n_g and sound pressure n_p level in function of the cavitation number σ, when testing a double-suction pump, at two different frequencies.

Variation des niveaux d'accélération n_g *et de pression sonore* n_p, *en fonction du* σ *de cavitation, correspondant à des essais faits sur une pompe à double aspiration et pour deux fréquences différentes.*

13/ Sound pressure level n_p in function of the cavitation number σ, for a wedge model, at different flow velocities v.

Niveau de pression sonore n_p *en fonction du* σ *de cavitation : modèle de coin et vitesse d'écoulement* v *variable.*

14/ Sound pressure p_h (mg/cm²) and the relative lengths characteristics of the cavitation conditions λ/l, λ_o/l, in function of the cavitation index k_d, according to Numachi [19].

Pression sonore p_h *(mg/cm²) et longueurs relatives caractéristiques du régime de cavitation* λ/l, λ_o/l, *en fonction de l'indice de cavitation* k_d, *d'après Numachi [19].*

15/ Variation of the sound pressure level n_p and output characteristics Q, n, M, η, in the function of the cavitation number σ, for a Francis turbine model.

Variation du niveau de pression sonore n_p *et des caractéristiques de sortie Q,* n, *M,* η, *en fonction du* σ *de cavitation, dans le cas d'un modèle de turbine Francis.*

16/ Photograph of a cavitation funnel vortex ($\sigma = 0.165$).
Vue d'un tourbillon de cavitation entonnoir ($\sigma = 0{,}165$).

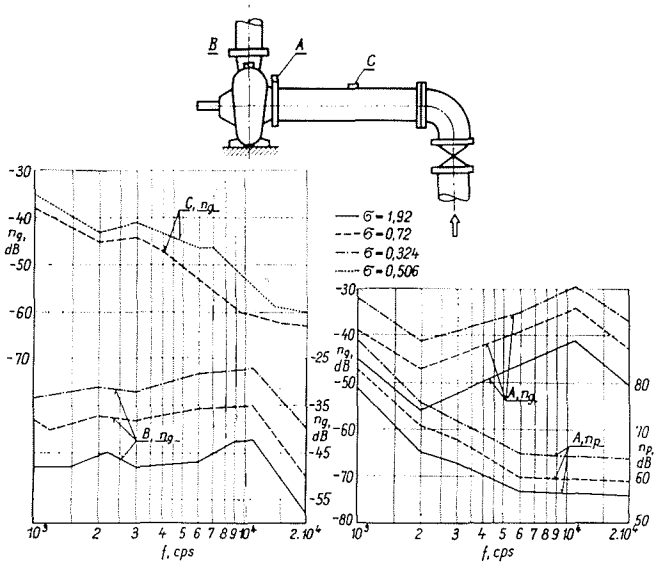

17/ Variation of the noise level n_p, n_g, in the function of frequency f, as measured at different points A, B, C, in pump tests, with constant cavitation numbers.

Variation du niveau sonore n_p, n_g, *en fonction de la fréquence* f, *mesurée à divers endroits (points A, B, C) au cours d'essais sur des pompes (σ constant).*

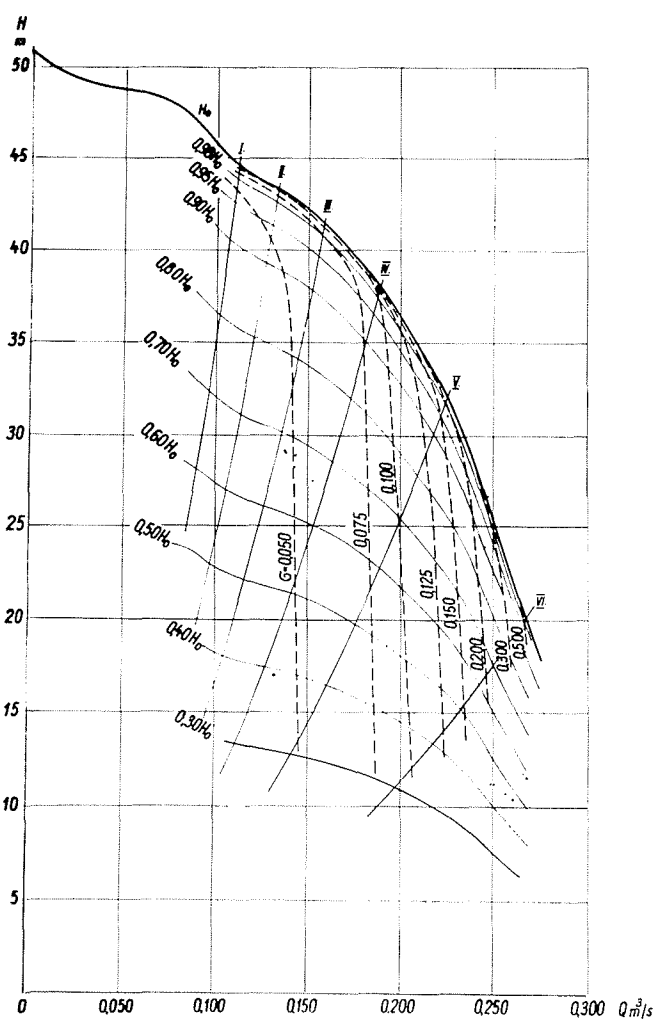

18/ Pump delivery head H in function of the pump delivery Q, with different cavitation numbers σ.

Hauteur de refoulement H d'une pompe en fonction du débit Q, avec un σ de cavitation variable.

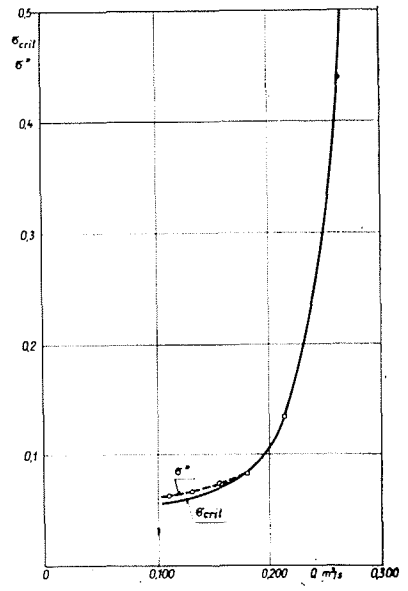

19/ Critical cavitation numbers $\sigma_{crit.}$ determined from delivery head measurement results, in function of the pump delivery Q. The points indicated represent the sigma values σ^* pertaining to the second noise level peak, as selected from the noise level n_g measurement results.

Sigma de cavitation critique, $\sigma_{crit.}$, *déterminé à partir de résultats de mesure de la hauteur de refoulement, en fonction du débit Q de la pompe. Les points indiqués représentent les valeurs de* σ^* *correspondant à la deuxième valeur maximale du niveau sonore, tirée des résultats des mesures du niveau sonore* n_g.

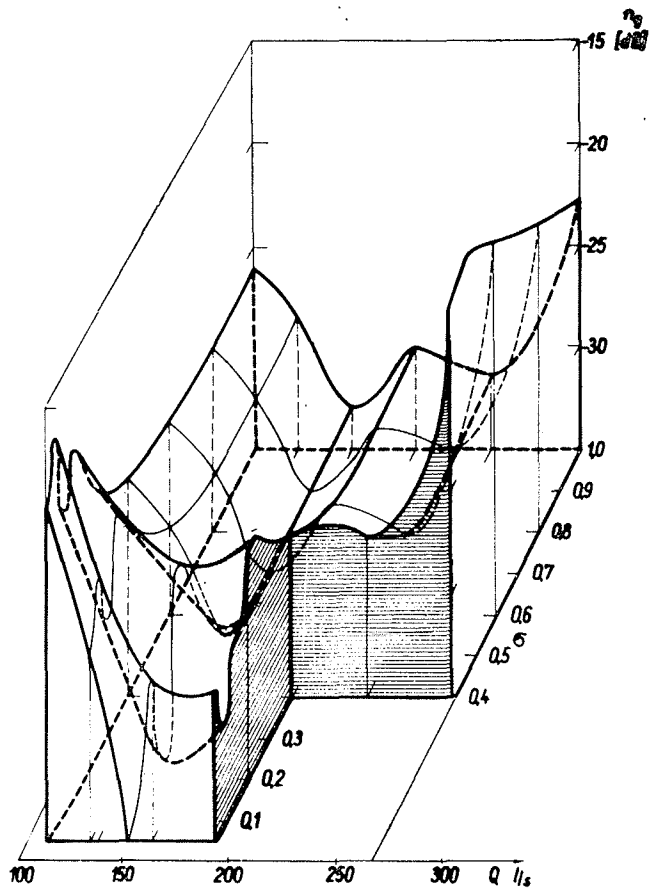

20/ Noise level surface; acceleration level n_g in function of the cavitation number σ and the pump delivery Q.

Surface du niveau sonore : niveau d'accélération n_g *en fonction du* σ *de cavitation et du débit Q de la pompe.*

ed from around $\sigma = 0{,}1$ on, as compared to the blade cavitation noise and, therefore, the lower section of the curve reflects the development and exhaustion of the blade cavitation. It could be established, furthermore, that the cavitation number pertaining to the peak value attributed to blade cavitation is very close to the point pertaining to the efficiency decrease. The development of two noise level curve peak values may be explained, therefore, by the development of cavitation at two different points in the turbine, where the peak value measured at a higher cavitation number is due to the cavitation funnel, and the one at the lower index is brought about by blade cavitation.

3. Noise level curves of pumps.

The pump noise level measurements involved semi open impeller (without front shroud) [9], closed impeller machines, and double suction pump [10]. First the effect of the various pick-up head locations was studied. The accelerometer was located first on the spiral casing, then at the suction pipe flange of the pump, and finally on the suction pipe proper, comparatively far away from the impeller. When tested under identical operating conditions, the noise spectra exhibited full agreement with the previous findings (Fig. 17).

The most detailed investigations involved a double entry pump featuring a characteristic speed of $n_q = 35$. The measurements were performed in a closed type test rig, at a constant speed, with a single measurement series under constant valve adjustment conditions, by gradually decreasing the internal pressure consequently along the curves marked I to VI on Figure 18. There were no possibility for the visual observation of cavitation, but the noise level measurements aimed exactly at obtaining information on the various cavitation conditions without visual observation. The noise level curves pertaining to one of the operating conditions are presented in Figure 12 referred to above. The two peak values of the noise level curves lead to the conclusion that two different cavitation types were produced in the pump whereof one was developed at a higher, and the other at a lower cavitation number. The σ_{crit} value defined by a 2 % reduction, of the head, representing the sudden decreasing of delivery head, exhibits good agreement with the cavitation number belonging to the second peak. Figure 19 illustrates the σ_{crit} values measured for different deliveries of the pump that coincided in each case with the cavitation number corresponding to the second peak of the noise level curve plotted. This reveals that the noise level measurements are suitable for the determination of the σ_{crit} value, with good approximation in case of this pump at least.

Figure 20 illustrates the noise level surface plotted in function of the volumetric flow Q and cavitation number σ. Such a presentation of noise level measurement results makes possible the uniform survey of the cavitation behaviour of the pump. The cavitation measurements on the pump can be performed along the different curves of the Q-H field (for example along the parabolae, if constant valve setting is used, or along the Q = Cte lines under the same conditions, etc.) and, accordingly, the noise level curves plotted along the different curves will depend on the measurement method employed, but the noise level surface will be independent thereof. The character of the noise level surface reveals, furthermore, that the nature of the noise level curves (the location of peaks) plotted along the different lines is identical.

V. — Noise level, noise intensity, and cavitation erosion

The test results described above show that, regardless of where the cavitation was produced, its noise level reflect a uniform character. The noise level curves make possible the determination of characteristic cavitation points for practical purposes with an acceptable safety, and they offer information on the cavitation of maximum intensity as well.

1. Noise level and cavitation erosion.

Previous investigations carried out with the cavitation tunnel confirmed [7] that the cavitation numbers pertaining to the noise level peaks or the relative cavity lengths were identical in both noise and cavitation erosion tests, that is, the maximum intensity of the cavitation erosion would appear at the point of maximum noise level (Fig. 9, 21 and 22).

In the course of cavitation erosion investigations, furthermore, it was ascertained that, under identical cavitation conditions, the relationship:

$$\Delta V = \beta v^5$$

holds good for the cavitation erosion intensity (rate of erosion) and the velocity of the flow. This is in full agreement with the acoustic test results discussed below.

2. Noise level and noise intensity.

The noise level curves presented in Figure 13 are approximately parallel, relatively located depending from the flow velocity, and it is easy to realize that, in case of a given cavitation number, the noise level would increase in conformity with the increase of the flow velocity. Using the data of this Figure, Figure 23 presents the noise level values pertaining to one of the cavitation conditions, in function of the logarithm of the flow velocity. On this Figure noise level values pertaining besides two different cavitation conditions are shown as well of results obtained with cylindrical model. Since, between intensity and sound pressure, the well-known equation $I = p^2/\rho c$ is existing, the exponent in the relationship of the intensity of the noise emitted and flow velocity:

$$I = \alpha v^m$$

may be determined from the straight lines on the Figure. Our test results show $m = 5$ as the probable velocity exponent value which conforms to the relation obtained for the intensity of the cavitation erosion. It seems to be confirmed by this, that in

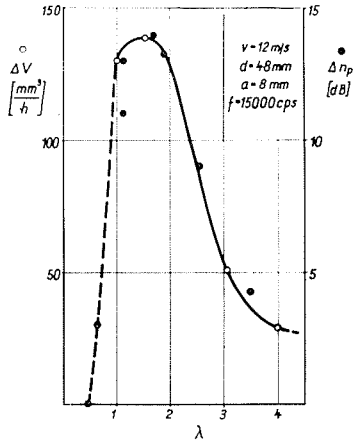

21/ Erosion intensity ΔV and noise level Δn_p in function of the extent of the cavitation conditions, according to cylinder model tests; a : tickness of the lead specimen.

Différences d'intensité d'érosion ΔV et de niveau sonore Δn_p, en fonction de l'étendue des conditions de cavitation, d'après des essais sur modèles cylindriques; a : épaisseur de l'échantillon en plomb.

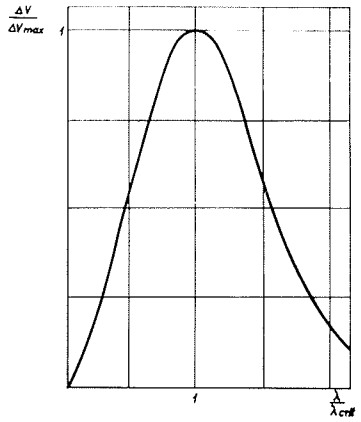

22/ Relative intensity of the cavitation damage $\Delta V/\Delta V_{max.}$, in function of the relative extent of the cavitation conditions $\lambda/\lambda_{crit.}$, according to erosion tests performed with cylinder models.

Intensité relative du pouvoir destructif de la cavitation $\Delta V/\Delta V_{max.}$, en fonction de l'étendue relative des conditions de cavitation $\lambda/\lambda_{crit.}$, d'après des essais d'érosion effectués sur modèles cylindriques.

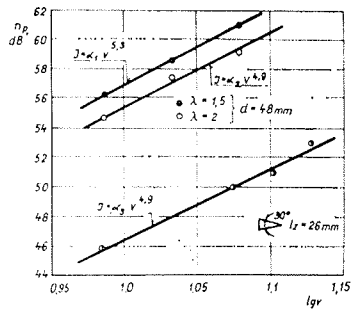

23/ Noise level n_p in function of the logarithm of flow velocity $\log v$, for circular cylinder and wedge model. Parameters : the length l_z and relative cavity length λ.

Niveau sonore n_p en fonction du logarithme de la vitesse d'écoulement log v, correspondant à des modèles de cylindre circulaire et de coin. Paramètres : longueur l_z et longueur de cavité relative λ.

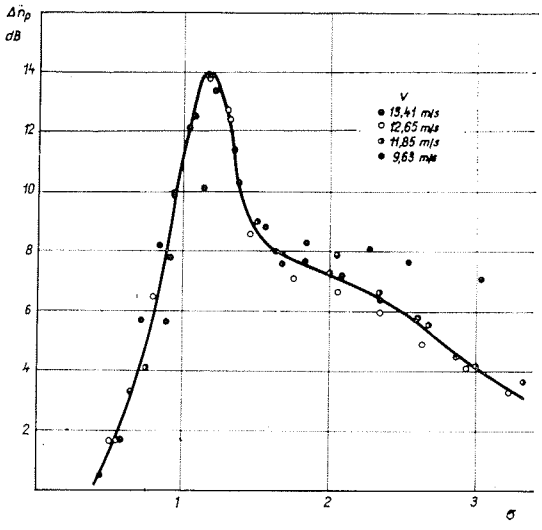

24/ Noise level differences converted to the $v = 12$ m/sec. velocity Δn_p^*, in function of the cavitation number σ, in case of a wedge model.

Différences du niveau sonore, Δn_p^*, ramenées à la vitesse $v = 12$ m/s en fonction du σ de cavitation, dans le cas d'un modèle cylindrique.

25/ Corrected noise level differences Δn_p^* in function of the extent of the cavitation condition λ, in case of a cylinder model.

Différences corrigées du niveau sonore Δn_p^*, en fonction de l'étendue de la condition de cavitation λ, dans le cas d'un modèle cylindrique.

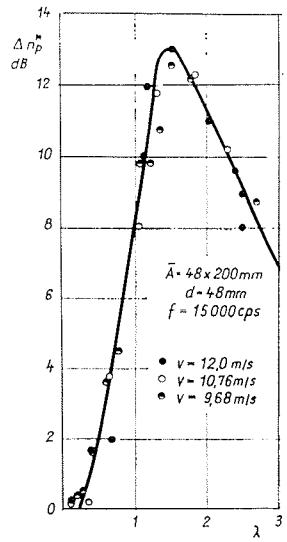

case of a given object there is a proportionality between the intensity of cavitation erosion and the intensity of noise emitted at a given cavitation number which is independent of the flow velocity.

The velocity exponent value for air-flows is according to Gerrard [20] $m = 4$, according to Stowell and Deming [21] $m = 5{,}5$, and Blokhintzev [22], Curle [23], as well as Etkin and al. [13] estimate it as $m = 6$. Börner [24] found an exponent of $m = 4$ for noises produced in turbulent flows, while the pump test results published by Pokrovsky and Yudin [17] point to a probable exponent of $m = 6$ to 7. These results are in conformity with the exponent $m = 5$ suggested.

The value of the velocity exponent ($m = 5$) may be applied generally for the results of the research. This exponent value was used to convert the noise level curves plotted with the various flow velocities presented in Figure 13 to the $v = 12$ m/s flow velocity (Fig. 24). Converting the noise level curves plotted for a cylindrical model, again to the $v = 12$ m/s flow velocity, rendered similar results (Fig. 25). Conversion made use of the formula

$$\Delta n_{p1}{}^* = \Delta n_{p1} - 10 \lg \left(\frac{v_1}{v_2}\right)^5$$

where Δn_{p1} is the noise level measured under given cavitation conditions pertaining to velocity v_1, as compared to a reference level, and $\Delta n_{p1}{}^*$ is the noise level converted to velocity v_2 related to the same reference level.

The above equation was used for the conversion of the noise level measurement results of the pump test illustrated by Figure 17. In course of the measurements, the pump speed varied between 500 and 1 450 rpm. Considering the peripheral velocity of

the impeller as that characteristic for calculation according to the formula given above it was converted (with an exponent of $m = 5$), to the speed of 1 000 rpm. The results of the conversion are presented in Figure 26. The examinations made possible the visual observation of cavitation and, accordingly, clearance cavitation inception began at $\sigma_i = 1{,}25$; with the differences between visual observation and noise measurements taken into consideration, the numbers found were in good agreement with the results read off the converted curve. The Figure verifies that the noise level curve pertaining to the constant speed can be determined with acceptable approximative accuracy from the noise level values measured at a variable speed, if the correction employed is made use of. It confirms, furthermore, the previous statement that the effect of Reynolds number variations is insignificant in these tests, and justifies the velocity exponent value adopted for the conversion.

In addition to emphasizing the close correlation between the cavitation conditions and the associated noise level as well as the cavitation erosion, then between the output characteristics of the hydraulic machines, their cavitation conditions, and the noise level, respectively, the test results described above lead to the conclusion that noise level measurements represent such a method whereby the cavitation behaviour of hydraulic machines can be determined indirectly.

VI. — Conclusions

The experiences collected through the multilateral application of the noise measurement techniques lead to the following conclusions:

Cavitational flow reflects two major noise generators, namely the noise of the periodic vortex separation, emitted at a discrete frequency determined by the flow conditions proper, and the noise radiated at a wide frequency spectrum produced by the collapse of the cavitation bubbles. From noise test aspects, the latter is of the more significant importance.

The noise spectra determined under various cavitation conditions depend, above a certain frequency limit, basically on the cavitation conditions which, in turn, provides for information on the state of cavitation from the noise level measurement results, with these measurements performed at any frequency within a predetermined interval. The appropriate frequency interval is that where the spectrum curves do not intersect one another, and where the measurement frequency selected is sufficiently far away from the frequency number of the noise of periodic vortex separation (Generally this interval is 6 000 ... 20 000 cps).

The noise level curve of isolated cavitation offers a basis for the determination of the inception development, and exhaustion of the cavitation proper, in an indirect manner.

Due to their simplicity, acceleration level measurements seem to be much more advantageous as compared to sound pressure level measurements, particularly because the location of accelerometers can be optionally selected, within certain reasonable limitations, on the object tested.

The noise (acceleration) level curves make possible to conclude approximately from noise intensity to flow velocity which is quite important with respect to the evaluation of the expected cavitation damage, since the extent of erosion varies with the fifth power of the velocity.

The intensity of cavitation erosion is in close correlation with the intensity of the noise and, consequently, it is possible to conclude from noise intensity to that of the cavitation damages.

The cavitation noise of hydraulic machines is produced, generally, by the superposition of the isolated cavitations brought about at different points. The noise level surface determined in function of the characteristic data exhibited by the hydraulic machines will comprehensively reflect the cavitation behaviour of the machine tested.

Under given cavitation conditions, noise intensity is proportional to the fifth power of velocity. On the basis of this fact, a noise level measured at a given velocity may be converted to other velocities as well which, in turn, makes possible the conversion of the noise level measurement results obtained at various hydraulic machines speeds to a constant speed value.

Symbols

a : the thickness of specimens used in erosion test;
c : sound velocity;
c_a : average flow velocity before the runner;
d : characteristic model dimension (diameter of the circular cylinder model);
f : frequency;
g : gravity acceleration;
g^* : acceleration of the measured vibrations;
l_z : visually observed length of the cavitation zone behind the model;

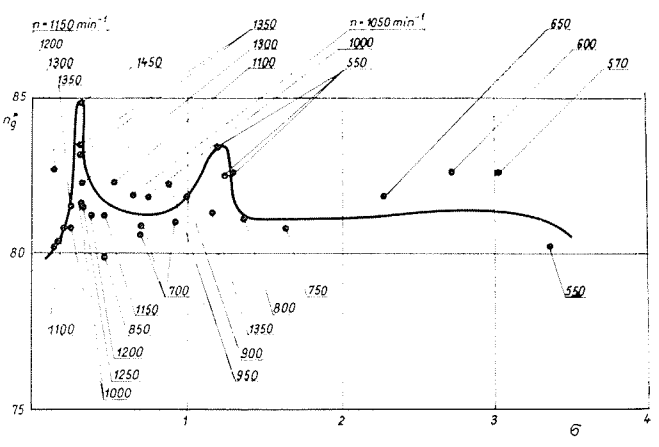

26/ Noise level converted to a speed of 1 000 rpm n_g^*, in function of the cavitation number σ, in case of a pump.

Niveau sonore n_g^* ramené à la vitesse de 1 000 tr/mn, en fonction du σ de cavitation, dans le cas d'une pompe.

m : flow velocity exponent;
n : speed (rpm);
n_g : acceleration level, $n_g = 10\ lg\ (g^*/g)^2$;
n_g^* : corrected acceleration level;
n_p : sound pressure level, $n_p = 10\ lg\ (p/p_0)^2$;
n_p^* : corrected sound pressure (noise) level;
n_s : specific speed of the turbine;
n_q : specific speed of the pump;
Δn_p : sound pressure level difference;
Δn_g : acceleration level difference;
p : sound pressure;
p_0 : basic sound pressure level;
p_s : absolute suction head upstream the impeller as related to the height of the axis;
p_v : vapor pressure pertaining to the given liquid temperature;
p_∞ : pressure measured at the sidewall, in the place of the model but in its absence;
v : mean velocity of undisturbed flow;
$\overline{A}$: profile size of the test section;
D : turbine runner diameter;
H : net head across machine;
H_b : barometric head;
H_0 : pump delivery head;
H^*_0 : delivery head pertaining to the water quantity actually delivered in cavitating condition, on the characteristic curve plotted for Q_0 (H_0) non-cavitation operation;
H_s : geometric suction head;
H_v : pressure head of the saturated water vapour;
I : intensity;
M : moment;
Q : volumetric flow through the machine;
Q_0 : volumetric flow measured under non-cavitating conditions;
$\mathcal{R}$: Reynolds number, $\mathcal{R} = vd/\nu$;
ΔV : erosion intensity (rate of erosion);
ΔV_{max} : maximum erosion intensity;
$\mathcal{S}$: Strouhal number, $\mathcal{S} = fd/v$;
α : proportion factor;
β : proportion factor;
γ : specific weight of the liquid;
η : efficiency;
λ : relative cavity length $\lambda = l_z/d$;
λ_{crit} : critical value of the relative cavity length;
ν : kinematic viscosity;
ρ : density;
τ : time;
σ : cavitation number:

for turbines:

$$\sigma := \frac{H_b - H_s - H_v}{H}$$

for pumps:

$$\sigma = \frac{\Delta h_{NPSH}}{H_0^*}$$

$$\Delta h_{NPSH} = \frac{p_s}{\gamma} + \frac{c_s^2}{2g} - \frac{p_v}{\gamma}$$

for model tests in a hydrodynamic tunnel:

$$\sigma = \frac{p_\infty - p_v}{(\rho/2)\ v^2}$$

σ_i : incipient value of cavitation;
σ_{crit} : critical value of the cavitation number;
σ^* : the sigma value pertaining to the second peak of noise level curve.

On Figures taken over from other authors, the symbols used by these authors are also adopted.

References

[1] Holl (J. W.) and Wislicenus (C. F.). — Scale Effects Cavitation. *Trans. ASME Journ. of Basic Eng.*, 83 (1961), 385.

[2] Williams (E. E.) and McNulty (P.). — Some Factors Affecting the Inception of Cavitation. Proc. Symp. on Cavitation in Hydrodynamics. NPL Teddington HMSO (1955), Paper No. 2.

[3] Lehmann (A. F.) and Young (J. O.). — Experimental Investigations of Incipient and Desinent Cavitation. *Trans. ASME Journ. of Basic Engineering*, 86 (June 1964), 275-281.

[4] Hammitt (F. G.). — Discussion of Lehmann and Young "Experimental Investigations of Incipient and Desinent Cavitation". *Trans. ASME Journ. of Basic Eng.*, 86 (1964), p. 281.

[5] Rata (M.). — Recensement et examen critique des méthodes d'observation de la cavitation par voie acoustique. *La Houille Blanche*, n° 6 (1963), 671-677.

[6] Cormault (P.). — Contribution à l'influence des teneurs en gaz de l'eau sur la cavitation dans les turbomachines hydrauliques. *Bull. Centr. Rech. et d'Essais de Chatou*, suppl. n° 2 (décembre 1962).

[7] Varga (J.) and Sebestyen (Gy.). — Cavitation Noise Spectrum and Cavitation Damage. *Acta Techn. Hung.*, 57, 3-4 (1967), 383-396.

[8] Varga (J.) and Sebestyen (Gy.). — Experimental Investigation of Cavitation Noise. *La Houille Blanche*, n° 8 (1966), 905-910.

[9] Sebestyen (Gy.), Stvrteczky (F.), Szabo (A.) and Verba (A.). — Contributions to Decide the Beginning of Cavitation in Pumps. *Acta Techn. Hung.*, 58, 3-4 (1967), 451-462.

[10] Sebestyen (Gy.), Fay (A.) and Csemniczky (I.). — Measurements of cavitation characteristics of a pump connected with measurement of noise. *Acta Techn. Hung.* (At press.)

[11] Sebestyen (Gy.) and Fay (A.). — Contributions to the Cavitation test on Francis Model Turbine. *Acta Techn. Hung.*, 60 (1968), 199-222.

[12] Pearsall (I. S.). — Acoustic Detection of Cavitation. Symp. on Vibrations in Hydraulic Pumps and Turbines. Manchester (Sept. 14-16, 1966), Paper 14, 1-8.

[13] Etkin (B.), Korbacher (G. K.) and Keefe (R. T.). — Acoustic Radiation from a Stationary Cylinder in a Fluid Stream. (Aeolian Tones.) *The Journ. of the Acoustical Society of America*, vol. 29, No. 1 (1957), 30-36.

[14] Varga (J.) and Sebestyen (Gy.). — Determination of the Frequencies of Wakes Shedding from Circular Cylinders. *Acta Techn. Hung.*, vol. 53, No. 1-2 (1966), 91-108.

[15] Varga (J.) and Sebestyen (Gy.). — Experimental Investigation of some Properties of Cavitating Flow. *Periodica Polytechnica Engineering*, vol. 9, No. 3 (1965), 243-254.

[16] Lecher (W. A.). — Cavitation observations and noise measurements as a means of investigating the trailing-edge vibration of turbine blades. I.A.H.R. Congress, London (1963), 3, 14, 109-116.

[17] **Покровский (Б. В) и Юбин (Е. Я.).** — Основные особенности шума и вибрации центробе жных насосов. Акустический Журнал; Т. XII. (1966) Вып. 3. 355-364.

[18] Silberman (E.) and Song (C. S.). — Instability of Ventilated Cavities. *Journ. of Ship Res.*, (June 1961), 13-33.

[19] Numachi (F.). — Ultraschallwelle am Tragfügelprofil bei Hohlsog. Teil III : *Rep. Inst. High Sp. Mech., Japan*, vol. 12 (1960-1961), Rep. No. 113, 63-87.

[20] Gerrard (I. H.). — Measurements of the Sound from Circular Cylinders in an Air Stream. *Proc. Phys. Society*, B 68 (1955), 453.

[21] Stowell (E. Z.) and Deming (A. F.). — Noise from Two-Blade Propellers. *Naca*, TN 526 (1935).

[22] **Блохинцев (Д. И.).** — Акустика неоднородной движущейся среды. Огиз-гостехиздат (1946).

[23] Curle (N.). — The influence of Solid Boundaries upon Aerodynamic Sound. *Proc. Royal Society of London*, 13 (1955), 505-514.

[24] Börner (H.). — Zur Schallentstehung in turbulenten Strömungen. *Acustica*, vol. 18 (1967), 151-158.

Résumé

La détection des phénomènes de cavitation à l'aide de méthodes acoustiques et de mesure des vibrations

par J.J. Varga *, G. Sebestyen ** et A. Fay ***

Les auteurs présentent une méthode de mesure acoustique permettant la détection, sous une forme simple et aisément reproductible, du caractère et de l'intensité des phénomènes de cavitation engendrés dans les machines hydrauliques, à des endroits normalement inaccessibles à l'observation visuelle. Le présent rapport réunit dans un cadre uniforme quelques résultats d'études antérieures, en les complétant avec les toutes dernières conclusions expérimentales. Les auteurs explicitent les résultats expérimentaux fondamentaux obtenus avec des modèles en tunnel de cavitation, et décrivent l'emploi de la méthode mise au point sur cette base pour le cas des modèles de turbine et de pompe. On constate que le spectre acoustique de la cavitation est indépendant des différents dispositifs de mesure, et de la nature des phénomènes de cavitation proprement dits, et présentant des caractéristiques uniformes. L'analyse de celles-ci fournit des données de base adéquates pour la mesure des niveaux sonores et pour la détermination des courbes correspondantes, en fonction de fréquences constantes d'une valeur bien déterminée. Le caractère des courbes définissant les niveaux sonores dépend avant tout de la variation des conditions de cavitation, ainsi qu'il a été vérifié au cours d'un nombre d'expériences différentes. Ces courbes des niveaux sonores permettent la détermination, à la fois des coefficients caractéristiques du seuil de cavitation, et des sections de développement ou d'épuisement des phénomènes de cavitation, ainsi que l'estimation du coefficient de cavitation caractéristique de la baisse de rendement. Les auteurs mettent en évidence l'étroite corrélation existant entre le niveau sonore de la cavitation et l'érosion, et confirment l'hypothèse suivant laquelle les conditions les plus dangereuses au point de vue de la cavitation seraient liées au coefficient de cavitation correspondant à une valeur maximale de la courbe des niveaux sonores. Enfin, on examine la transposition de ces courbes en fonction de différentes vitesses d'écoulement, ou de rotation, de la pompe à l'aide de la corrélation existant entre le niveau sonore et les vitesses d'écoulement.

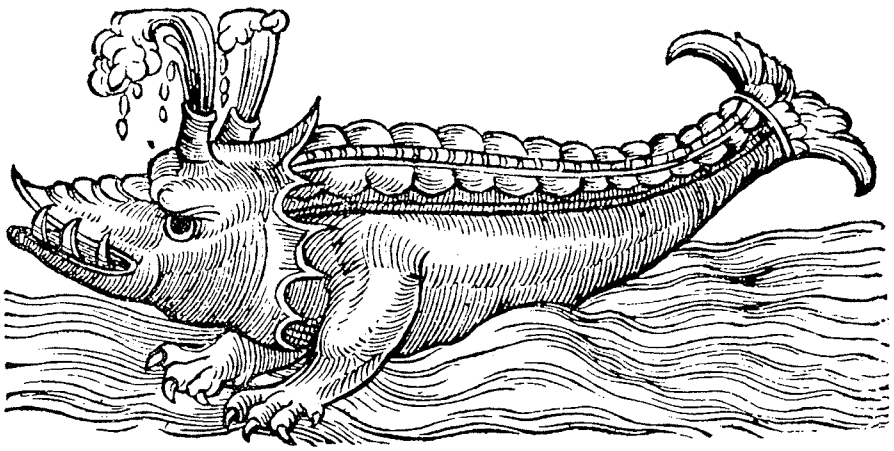

Bois gravé du XVI^e siècle

* Professor, Department of Hydraulic Machinery, Budapest Technical University (Hungary).

** Research Engineer, Department of Hydraulic Machinery, Budapest Technical University (Hungary).

*** Mech. Eng., Math., Department of Hydraulic Machinery, Budapest Technical University, and Ganz-Mavag Co, Budapest (Hungary).

Gravure extraite de Architectura curiosa nova *par G. A. BOCKLERN*
Nuremberg (1664)